

Bose-Einstein Condensation in a CO₂-laser Optical Dipole Trap

Giovanni Cennini, Gunnar Ritt, Carsten Geckeler, and Martin Weitz

Physikalisches Institut der Universität Tübingen, Auf der Morgenstelle 14, 72076 Tübingen, Germany

Received: date / Revised version: date

Abstract We report on the achieving of Bose-Einstein condensation of a dilute atomic gas based on trapping atoms in tightly confining CO₂-laser dipole potentials. Quantum degeneracy of rubidium atoms is reached by direct evaporative cooling in both crossed and single beam trapping geometries. At the heart of these all-optical condensation experiments is the ability to obtain high initial atomic densities in quasistatic dipole traps by laser cooling techniques. Finally, we demonstrate the formation of a condensate in a field insensitive $m_F = 0$ spin projection only. This suppresses fluctuations of the chemical potential from stray magnetic fields.

1 Introduction

Since the first observation of Bose-Einstein condensation (BEC) in a dilute atomic gas, we have been witnessing dramatic progress in both theoretical and experimental studies of degenerate quantum gases [1, 2]. A variety of static and dynamic properties of the condensed, trapped atoms have been exploited [3]. Interference studies with Bose-condensates have experimentally demonstrated the coherence properties expected for such a ‘giant matter wave’ [2]. More recently, the Mott-insulator phase transition has been observed by loading a magnetically trapped condensate into a steep optical lattice [4].

The standard approach to produce a Bose-Einstein condensate involves a laser cooling of the atomic sample to a phase space density of 10^{-6} , after which atoms in weak-field seeking states are transferred into a magnetic trap [1, 2]. Further cooling proceeds by a radiofrequency field selectively transferring the highest energetic atoms into untrapped states, which evaporatively cools the atoms to quantum degeneracy. A drawback of magnetic traps is that they only confine weak field seeking spins states, which e.g. prevents one from studying spinor condensates directly in these traps [2]. Moreover, atoms in field independent $m_F = 0$ spin projections, as

are of large interest for many precision experiments [5], cannot be confined in magnetic traps.

Far detuned optical dipole traps can confine atoms in arbitrary spin states. Dipole traps furthermore allow for very variable trapping geometries, as e.g. periodic lattice geometries. Experiments aiming at an achieving of quantum degeneracy in optical dipole traps have been first carried out by the Stanford group [7]. In far detuned dipole traps, a variety of refined optical and evaporative cooling techniques have been implemented, which has allowed for atomic phase space densities very close to quantum degeneracy [6]. Friebel et al. found that in quasistatic dipole traps, as can be realized with a CO₂-laser, polarization gradient cooling alone can accumulate atoms to a phase space density three orders of magnitude above that of a conventional MOT [8]. Chapman and coworkers have reported on the observation of Bose-Einstein condensation by direct evaporative cooling in a crossed CO₂-laser dipole trap [10]. All-optical cooling techniques have also enabled the first observations of quantum degeneracy of ⁶Li, cesium and ytterbium atoms [11, 12, 13].

We here describe experiments creating rubidium Bose-Einstein condensates by direct evaporative cooling in both a crossed and a single beam quasistatic dipole trapping geometry [14]. Due to the choice of a tight trapping laser focus, stable evaporation to a Bose-Einstein condensate is possible in both geometries even with moderate initial number of atoms. Especially the single dipole trapping geometry allows for a considerable experimental simplification of methods to produce Bose-condensed atoms. Note that previous experiments realizing quantum degeneracy in dipole traps have either required a more alignment sensitive crossed beam geometry or Feshbach resonances to enhance the collisional rate [10, 11, 12, 13]. By applying a magnetic field gradient to the single beam configuration, we realized a trap stable for atoms in a field insensitive $m_F = 0$ spin projection only. In a recent work, this has enabled us to realize an all-optical atom laser [15]. The chemical potential of the

generated condensate is first order insensitive to fluctuations from stray magnetic fields.

2 Quasistatic Optical Dipole Traps

Optical dipole traps for atoms are based on the force which arises from the coherent interaction between the induced atomic dipole moment and the laser electric field [17, 18]. When the laser frequency is tuned to the red side of an atomic resonance, the dipole force pulls atoms towards the intensity maxima of the field. For optical fields with frequency far below all electric dipole resonances of ground state atoms (i.e. ‘quasistatic’ fields), the trapping potential is given by

$$U = -\frac{1}{2}\alpha_s |\mathbf{E}|^2 \quad (1)$$

where α_s denotes the static atomic polarizability of the electronic ground state and \mathbf{E} is the electric field of the optical wave. For the ground state and the first excited state of the rubidium atom, the scalar static polarizability is $\alpha_{5S} = 5.3 \times 10^{-39} \text{ m}^2\text{C/V}$ and $\alpha_{5P} = 1.3 \times 10^{-38} \text{ m}^2\text{C/V}$, respectively [19]. Since the frequency of the CO₂-laser radiation (λ is near 10.6 μm) used in our experiment is approximately one order of magnitude below that of a typical electric dipole transition of ground state alkaline atoms, the photon scattering rate is very small. In particular, the Rayleigh photon scattering rate in this quasistatic regime is given by the expression

$$\Gamma_s = \frac{16r_0^2 P}{3\hbar w_0^2} \left(\frac{m_e \alpha_s}{e^2} \right) \omega^3 \quad (2)$$

where w_0 is the beam waist of a laser beam with power P , r_0 the classical electron radius, m_e the electron mass and ω denotes the optical frequency of the laser light. In our experiments, the Rayleigh scattering rate of trapped rubidium atoms is of the order of 1/600 s. This results in a small coupling of the atoms to the environment, so that the effect of decoherence can be kept small. Let us note that for alkali atoms trapped in an extremely far-detuned laser field, the detuning from resonance is much larger than both the hyperfine and fine structure splitting. This condition is met in our quasistatic trapping field. The trapping potential for ground-state alkali atoms here corresponds to that of a $J = 0$ to $J' = 1$ transition, and the ac Stark shift for all ground-state sublevels is almost identical. This state-independent confinement of extremely far-detuned optical dipole traps for many experiments represent an advantage over magnetic traps. It is however clear that evaporative cooling cannot be achieved by selectively transferring atoms into untrapped states, as usually done in magnetic traps. Such a cooling in optical traps can be achieved by lowering the intensity of the trapping beams in a controlled way, which decreases the depth of trapping potential [7].

3 Experimental setup and procedure

A scheme of our experimental setup used for direct Bose-Einstein condensation of rubidium atoms in a dipole trap is shown in Fig. 1. A commercial, rf-excited single mode CO₂-laser generates up to 50 W mid-infrared radiation near 10.6 μm . The light passes two acousto-optic modulators (AOMs). The first one allows us to regulate the laser beam intensity via controlling of the rf-drive power. The light diffracted in first order from this modulator passes a second AOM, whose function is that of a beam divider for the crossed beam experiments. Note that the zero’s and first order diffracted beams differ in frequency, which eliminates unwanted standing-wave effects. The mid-infrared beams enter a vacuum chamber through ZnSe windows. For each beam, an adjustable, spherically corrected ZnSe lens ($f = 38.1 \text{ mm}$) placed inside the vacuum chamber focuses the laser beams to a minimum waist size of 20 μm . The beam focus can be varied with a telescope located outside of the vacuum chamber. For the crossed trap geometry, a beam waist of 35 μm is chosen, whereas for a single running wave geometry we use a beam size of 27 μm in the trapping region. For the former geometry, the trapping beams are directed horizontally and vertically respectively and cross each other with a 90 degree angle. For the single beam trapping geometry, the second AOM is omitted and the transmitted beam travels through the vacuum can in horizontal direction.

Atoms of the isotope ⁸⁷Rb are initially collected and pre-cooled in a magneto-optical trap (MOT), which is loaded from the thermal gas emitted by heated rubidium dispensers. The measured background gas pressure inside the vacuum chamber is 1×10^{-10} mbar. The near-resonant radiation for cooling and trapping atoms in the MOT is generated by grating stabilized diode lasers. A cooling laser operates with variable red detuning from the closed $5S_{1/2}$, $F = 2$ to $5P_{3/2}$, $F' = 3$ hyperfine component of rubidium D2-line. Its radiation is amplified by a second injection locked free-running diode laser. In order to repump rubidium atoms into the cooling cycle, a second grating-stabilized diode laser locked to the $5S_{1/2}$, $F = 1$ to $5P_{3/2}$, $F' = 2$ transition is employed. Both cooling and repumping light beams pass acousto-optic modulators and are spatially filtered. These near-resonant beams are expanded to a beam diameter of 20 mm, spatially overlapped and then directed to the vacuum chamber to provide three retroreflected MOT beams. The total optical power of the cooling light after spatial filtering is 42 mW, whereas that of the repumping light is 9 mW. We use a pair of magnetic coils oriented in anti-Helmholtz configuration to generate a magnetic quadrupole field with a 10 G/cm field gradient, whose center is close to the intersection of the two CO₂-laser beams. The coil axes is oriented at an angle of 45 degree with respect to the vertical and horizontal

CO₂-laser beams. This quadrupole field is e.g. used to operate the MOT.

An experimental cycle begins by loading the magneto-optical trap. During the course of the experiment, we have used different MOT loading times. A typical value for e.g. the earlier crossed beam dipole trapping experiments is 1×10^7 trapped atoms in the MOT accumulated during a 5 s loading time. During this MOT loading phase, the cooling laser operates with a red detuning of 18 MHz to the red of the cycling transition. Subsequently, we increase the detuning of the cooling laser to a value of 160 MHz and simultaneously reduce the repumping laser intensity by a factor 100 for a 60 ms long time interval. In this temporal dark MOT phase (d-MOT)[20], the atoms are pumped into the lower hyperfine state ($F = 1$), which reduces hyperfine changing collisions. These quoted parameters are optimized by maximizing the number of atoms transferred to the dipole trap. Throughout this cycle the CO₂-laser radiation is left on, allowing for rubidium atoms to accumulate in the dipole trapping region. At the end of the d-MOT phase, the repumping light is extinguished and after a delay of 2 ms also the cooling light. Simultaneously, the magnetic quadrupole field is switched off. By this time, the atoms are confined by the quasistatic dipole trap alone. All near-resonant beams are carefully extinguished by both AOMs and mechanical shutters. The small delay between the extinguishing of repumping and cooling light minimizes losses in the dipole trap due to hyperfine changing collisions.

To analyze the properties of trapped atomic clouds, we employ the technique of absorption imaging. At the end of an experiment cycle, the trapped atoms are released by switching off the CO₂-laser beams. After a variable expansion time (typically 5–20 ms), cold atoms are irradiated with a pulse of light tuned resonantly to the $F = 2$, $F' = 3$ component of the rubidium D2 line. For this measurement, we use a spatially filtered laser beam with a 8 mm beam diameter. The beam is then imaged onto a slow-scan CCD camera, where shadow images of the atomic cloud are recorded. From these images, both number of atoms and atomic temperatures are extracted. The pulse length is 80 μ s and the intensity (100 μ W/cm²) is chosen to be clearly below saturation intensity. During this detection time, repumping light is provided by the MOT beams.

4 Experimental Results

4.1 Bose-Einstein condensation in a crossed beam geometry

In initial experiments, we studied BEC in a crossed beam geometry, similarly as done in work by Chapman et al. [10]. To reach Bose-Einstein condensation by direct evaporative cooling in our dipole traps, the initial phase

space density of the laser cooled clouds is first optimized. We have characterized the trap lifetime, trap frequencies and the temperature of the trapped atomic cloud. The vibrational frequencies are measured by periodically modulating the optical confining power with the first AOM, which allows us to study parametrically excitation of the trapped atoms [21]. Significant trap loss is observed when the modulation frequency is close to twice a trap vibrational frequency. With typical parameters of 12 W optical power in each of the CO₂-laser trapping beams and a 35 μ m waist radius, we observe parametric resonance corresponding to a vibrational frequency of $\nu = 1.7$ kHz. For this crossed beam geometry, the oscillation frequencies in the central trap region in all three spatial directions are similar. The trap lifetime is extracted by monitoring the number of atoms detected after different trapping times for a constant potential depth. A typical result of such a measurement is shown in Fig. 2a. The data points are taken after a minimum dipole trapping time of 70 ms, since for shorter delay times atoms not being transferred to the dipole trap have not yet been removed completely from the detection region by gravity. The data can be described with a two time constants exponential decay, which involves a fast and a slow decay with time constants near 100 ms and 12 s respectively. The fast decay in the beginning of the dipole trapping phase is attributed to a plain atomic evaporation of the highest energetic atoms. In contrast, the slow decay is attributed to losses due to collisions with background gas, which ultimately limit the available trapping time. Fig. 2b shows the dependence of the atomic temperature on trapping time. The temperature clearly decreases with time, which we attribute to the plain evaporation. This process is effective only for small trapping times when the loss rate is large. The measured atomic density after a trapping time of 500 ms is 1×10^{13} atoms/cm³. Together with the measured temperature of 60 μ K we derive a phase space product $n\lambda_{\text{dB}}^3 \simeq 1/500$, which corresponding to a 1/1500 phase space density if we assume equal distribution of spin projections. These results are comparable to previous results observed in CO₂-laser optical lattice and crossed dipole geometries [8]. We also infer a collisional rate of 7 kHz at this time, clearly representing a favorable starting point for further, forced evaporative cooling to lower temperatures. To induce such a forced evaporation, the optical potential is lowered in a controlled way. Experimentally, this is achieved by reducing the trapping laser beam intensity via a decreasing the rf-drive power of the first AOM. Mandatory for the success of evaporative cooling is to maintain a relatively high atomic collision rate, so that the remaining atoms can rethermalize to a distribution of lower temperature. We reduce the potential depth with time according to the formula

$$U(t) = U_0(1 + t/\tau)^{-\beta}, \quad (3)$$

where U_0 denotes the value of the initial potential depth. It was shown in Ref. 10 that this ramp form maintains a nearly constant ratio $\eta = U/k_B T$ between potential depth and the atomic temperature. Following a 100 ms long plain evaporation period, the mid-infrared power is reduced in a 3.5 s long ramp time from initially 12 W to a final value of 75 mW in each of the trapping beams. In these crossed dipole experiments, we find optimum cooling when choosing the parameters of Eq. (3) to be $\tau = 0.3$ s and $\beta = 1.5$. We have experimentally verified that the cutoff parameter η was nearly constant throughout the evaporation ramp. For a characterization of the cooling, we have analyzed shadow images of the expanded atomic cloud at the end of the evaporation process. Fig. 3a shows a cross-section of such an image for a final trapping power of 150 mW, corresponding to an average trap vibrational frequency of 350 Hz. It is clear that here the ensemble is still purely thermal. The phase space density is further increased when we ramp to lower power values. Fig. 3b shows data recorded for a final beam power of 100 mW, where a typical bimodal distribution corresponding to an atomic cloud near the transition point is observed. The central feature corresponds to atoms in the Bose-condensate, while the wings represent thermal atoms. The critical temperature here is $T_c = 190$ nK. For final power of 75 mW, an almost pure condensate is obtained as shown in Fig. 3c. The condensate contains about 10000 atoms distributed among the three m_F states of the electronic hyperfine ground state $F = 1$. In other measurements, we have applied a magnetic quadrupole field during the course of the evaporation by leading on the MOT coils. This leads to a condensate with about 70 percent population in the $m_F = 1$ and 30 percent in the $m_F = 0$ spin projection. For these trap parameters, the magnetic field gradient predominantly populates one field-sensitive state. In earlier work in a crossed dipole trap it was demonstrated that with different field gradients also other spin states can be populated, although it was noted that by the time of writing the origin of the obtained magnetization still remained to be determined [16].

4.2 BEC in a single running wave trap

In this chapter, we describe our experiments successfully creating a rubidium Bose-Einstein-condensate in a single beam CO₂-laser dipole trap. This is the simplest possible dipole trapping geometry. The use of single running wave allows for a compact setup and a very reliable production of the BEC. Previous experiments creating quantum degeneracy in dipole traps have either required the use of a more alignment-sensitive crossed dipole trap geometry [10, 13] or Feshbach resonances [12] to enhance the collisional rate during the course of the forced evaporation.

As in the case of the crossed dipole trap configuration, evaporative cooling towards BEC requires a ramp-

ing down of the trapping potential. Since the average of the trap vibrational frequencies for a given power and beam waist is smaller than in the crossed beam geometry, it is *a priori* not clear that the rethermalization rate is sufficiently high throughout the evaporation ramp. Obviously, the final stages of evaporation here are most critical, since the collisional rate decreases with trap power. It is easy to show that the trap vibrational frequencies in a single dipole trap orthogonal to the beam axis scale as $\nu_r \propto \sqrt{P}/w_0^2$, while along the beam axes scale as $\nu_z \propto \lambda\sqrt{P}/w_0^3$, where λ is the laser wavelength. Our experiments demonstrate, that by choosing a sufficiently small beam waist, the collisional rate can be high enough throughout the ramp, and BEC can be reached. For the single beam geometry, the focus of the (horizontally oriented) trapping beam is reduced to a 27 μ m beam waist. In principle, one could work with an even tighter focus to fully compensate for the smaller compression in this geometry. In our experiments, we have instead started with a higher number of atoms and also used a slightly longer evaporation time. The weak confinement along the beam axis of the single dipole trap geometry offers the additional benefit that it allows us to remove atoms in field sensitive spin projections with a moderate magnetic field gradient. We note that an alternative to such a state selection is to achieve field-insensitivity by using of atoms with a spin singlet ground state, as e.g. atomic ytterbium. Very recently in an impressive experiment, evaporative cooling in a crossed dipole trap has allowed for the production of a Bose-Einstein condensate of these atoms [13].

For our single dipole trap experiments, we increase the MOT loading time to 30 s, during which 6×10^7 are captured. At the end of the MOT loading, we apply a temporal dark-MOT phase as described in the above section. Subsequently, all near-resonant optical beams are extinguished and the atoms are trapped in the quasistatic dipole trapping potential alone. Typically, 4×10^6 atoms are captured in the single beam trap. We have characterized the vibrational frequencies of the trap. At full trapping laser power (28 W), we measure $\nu_r = 4.8$ kHz and $\nu_z = 350$ Hz, corresponding to vibrations orthogonal and collinear respectively to the beam axes. In this single beam geometry, there is no spherical symmetry and the longitudinal trap frequency is about 13 times smaller than the radial one. We again have first analyzed the trapping of atoms while maintaining full CO₂-laser trapping power. Following a 100 ms long plain evaporation phase, we measure an atomic temperature of 140 μ K and an atomic density of $n \simeq 1.2 \times 10^{13}$ atoms/cm³. This corresponds to a product $n\lambda_{dB}^3 \simeq 1.2 \cdot 10^{-4}$. Although this value is below best values obtained in quasistatic crossed dipole trap configurations or optical lattices, it is clearly above results achieved in magnetic traps prior to forced evaporative cooling. From the above values, we derive a high collision rate of 6.2 kHz. This has encouraged us to pro-

ceed with forced evaporative cooling in this single beam dipole trapping geometry.

To cool the atoms towards lower temperatures, we apply a 7 s long forced evaporation ramp, during which the power of the dipole trapping beam is reduced from its initial value of 28 W to a final value of 200 mW. This ramp is applied directly after the dark MOT phase, as for this geometry no improved cooling is observed when an initial plain evaporation phase is added. We again use a ramp form as described by Eq. 3. Optimum cooling in the single dipole trap was observed when using parameters τ and β near 0.45 s and 1.4 respectively. We have recorded time-of-flight (TOF) shadow images of the atomic cloud for different free expansion times. For this measurement, the MOT quadrupole field was switched off after the d-MOT phase. Fig. 4a shows an image recorded directly after switching of the trap laser, i.e. with no free expansion. The trapped cloud is cigar shaped and strongly elongated along the weakly confining beam axis. Figs. 4b and 4c give time of flight images recorded after a 8 ms and 15 ms respectively long free expansion phase. In the former image the cloud is almost symmetric, while in the latter image the symmetry axis is inverted. We interpret this series of images as a clear evidence for Bose-Einstein condensation in the single beam optical trap. In this asymmetric trap geometry, the cloud expands faster along the radial than along the axial direction due to the anisotropic release of mean field energy. The formed condensate has spinor nature. To analyze the distribution of Zeeman components, we apply a Stern-Gerlach magnetic field gradient during the free expansion phase, which spatially separates the different Zeeman components. Fig. 5a shows a typical measurement, where a separation into clouds with different spin projections is clearly visible. We produce condensates with typically 12000 atoms distributed among the $m_F = -1, 0, 1$ Zeeman components of the $F = 1$ ground state. As stated above, one of the main advantages of optical dipole traps is their state independent trapping, which allows for the formation and confinement of spinor condensates.

In subsequent experiments, we have condensed atoms in the $m_F = 0$ spin projection only. For this measurement, the magnetic quadrupole field generated by the MOT coils was left on throughout the experimental cycle, i.e. also during both dipole trapping and detection phases. For our experimental parameters, stable trapping of atoms during the final phase of the evaporative cooling is then only possible for the field insensitive ($m_F = 0$) spin projection. Atoms in spin projections $m_F = \pm 1$ are removed during the course of evaporative cooling by the field gradient (note that the dipole trap does in general not exactly overlap with the center of the quadrupole field). Fig. 5b shows a typical obtained time-of-flight shadow image of the condensed cloud. The measurement shows that only the $m_F = 0$ Zeeman state is populated. We typically obtain 7000 condensed atoms in

this first order field-insensitive state. Note that this number is larger than the obtained $m_F = 0$ fraction of the above discussed spinor condensate, which we attribute to sympathetic cooling with atoms in $m_F = \pm 1$ spin projections during condensate formation. The critical temperature of the $m_F = 0$ condensate is $T_c \simeq 220$ nK, and the peak-density is $1.2 \times 10^{14}/\text{cm}^3$. For both the spinor and the $m_F = 0$ condensate we measure condensate lifetimes near 5 s. This value is shorter than the inverse loss rate due to background gas collisions, and we attribute this lifetime to be mainly limited by three-body losses. Within our experimental uncertainty, we do not observe any difference between the lifetimes of a spinor and the $m_F = 0$ condensate. Further, we do not observe transfer of atoms from $m_F = 0$ state into field-sensitive states. To our belief, spin changing collisions here are suppressed by the quadratic Zeeman shift in the inhomogeneous magnetic field [22, 23].

5 Conclusions and Outlook

We have investigated Bose-Einstein condensation of rubidium atoms by direct evaporative cooling in tightly confining, quasistatic dipole traps. The quantum degenerate regime has been reached both in a crossed beam and a single beam CO₂-laser dipole trapping geometry. The former configuration allows cooling to quantum degeneracy with a somewhat larger trap focus. On the other hand, the newly developed single beam approach towards Bose-Einstein condensation provides a simpler setup and is less alignment sensitive. The scheme provides a very stable route towards the achieving of quantum degeneracy. Finally, we demonstrated that in the single beam setup a moderate magnetic field gradient yields a trapping configuration, in which stable confinement is possible only for atoms in a $m_F = 0$ spin projection. The chemical potential of the produced Bose-Einstein condensate is first order insensitive to stray magnetic fields.

For the future, we believe that the demonstrated single beam method for producing Bose-Einstein condensates due to its technical simplicity opens up wide applications in the physics with quantum gases. Further research could investigate an extension to the Bose-Einstein condensation of other atomic species, as e.g. alkaline-earth atoms.

Further, we anticipate the described method to produce condensates in a field-insensitive spin state can have impact on the application of quantum degenerate atoms to precision measurements, as e.g. atomic clocks or atom interferometry experiments. One can furthermore envision experiments with two-component quantum degenerate gases driven by exciting the microwave clock transition between the hyperfine ground states $F = 1, m_F = 0$ and $F = 2, m_F = 0$. It clearly remains important to study the stability of different spin projections against spin changing collisions in more detail.

Quasistatic optical dipole traps are of large interest for quantum computation. In a CO₂-laser lattice geometry the lattice spacing is so large that individual sites can be optically resolved, which allows for an individual addressing of qubits [24]. By inducing a Mott insulator phase transition, unity occupation of atoms in lattice sites can be achieved. An entanglement of atoms in the lattice is e.g. possible by cold, controlled collisions [25].

This work has been supported in parts by the Deutsche Forschungsgemeinschaft, the Landesstiftung Baden Württemberg, and the European Community.

References

1. See e.g.: E. A. Cornell and C. E. Wieman, *Rev. Mod. Phys.* **74**, 875 (2002).
2. See e.g.: W. Ketterle, *Rev. Mod. Phys.* **74**, 1131 (2002).
3. See e.g.: F. Dalfovo, S. Giorgini, L. P. Pitaevskii and S. Stringari, *Re. Mod. Phys.* **71**, 463 (1999).
4. M. Greiner, O. Mandel, T. Esslinger, T.W. Hänsch, and I. Bloch, *Nature* **415**, 39 (2002).
5. See e.g. articles in P. Gill, *Frequency Standards and Metrology* (World Scientific, Singapore, 2002).
6. A. J. Kerman, V. Vuletić, C. Chin, and S. Chu, *Phys. Rev. Lett.* **84**, 439 (1999); D. J. Han, S. Wolf, S. Oliver, C. Mc.Cormick, M. T. DePue, and D. S. Weiss, *Phys. Rev. Lett.* **85**, 724 (2000); T. Ido, Y. Isoya, and H. Katori, *Phys. Rev. A* **61**, 061403 (R) (2000).
7. C.S. Adam, H. Jin Lee, N. Davidson, M. Kasevich, and S. Chu, *Phys. Rev. Lett.* **74**, 3579, (1995).
8. S. Friebe, R. Scheunemann, J. Walz, T.W. Hänsch and M. Weitz, *Appl. Phys. B* **67**, 699 (1998).
9. See e.g.: R. Grimm, M. Weidemüller, and Y. B. Ovchinnikov, *Adv. At. Mol. Opt. Phys.* **42**, 95 (2000).
10. M. D. Barrett, J. A. Sauer, and M. S. Chapman, *Phys. Rev. Lett.* **87**, 010404 (2001).
11. S. R. Granade, M. E. Gehm, K. M. O'Hara, and J. E. Thomas, *Phys. Rev. Lett.* **88**, 120405 (2002).
12. T. Weber, J. Herbig, M. Mark, H. C. Nägerl, and R. Grimm, *Science* **299**, 232 (2003).
13. Y. Takasu, K. Maki, K. Komori, T. Takano, K. Honda, M. Kumakura, T. Yabuzaki, and Y. Takahashi, *Phys. Rev. Lett.* **91**, 0404041 (2003).
14. Our crossed dipole work was first reported at the 67. Physikertagung und AMOP-Frühjahrstagung, Hannover 2003; see also: G. Cennini, G. Ritt, C. Geckeler, and M. Weitz, *Verhandl. DPG (VI)* **38**, (2003).
15. G. Cennini, G. Ritt, C. Geckeler, and M. Weitz, [cond-mat/0307620](https://arxiv.org/abs/cond-mat/0307620)
16. M.D. Barrett, M. S. Chang, C. Hamely, K. Fortier, J. A. Sauer, and M. S. Chapman, in "Proceedings of the XVIII International Conference on Atomic Physics", H.R. Sagehpour, E.J. Heller, and D.E. Pritchard (eds.) (World Scientific, 2003).
17. S.Chu, J.E. Bjorkholm, A. Ashkin, and A. Cable, *Phys. Rev. Lett.* **57**, 314 (1985).
18. C. Cohen-Tannoudji, "Atomic Motion In Laser Light", In: *Les Houches, Session LIII* 1990, ed. by J. Dalibard, J.M. Raimond and J. Zinn-Justin (North Holland, Amsterdam 1992).

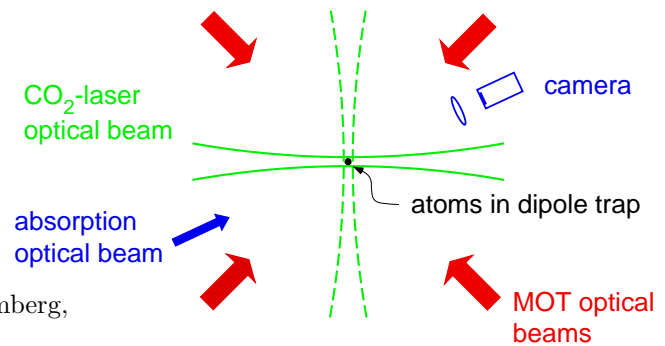


Fig. 1 Scheme of experimental setup

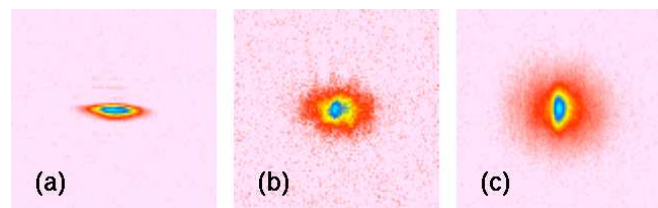


Fig. 4 Free expansion of a Bose-Einstein condensate generated in a single beam dipole trap. Shown is a series of shadow images of the atomic cloud recorded after allowing for different free expansion times (field of view $240 \mu\text{m} \times 240 \mu\text{m}$). (a) Image taken with nearly no free expansion, showing thus the cigar-shaped spatial distribution of the trapped cloud. (b) and (c): Recorded after a 8 ms and 15 ms respectively of free expansion. Especially at the latter time, the asymmetry of the cloud is inverted.

19. D.R. Lide, *CRC Handbook of Chemistry and Physics* (CRC Press, Boca Raton 1990); R. Marrus, D. McColm, J. Jellin, *Phys. Rev.* **147**, 55 (1966).
20. W. Ketterle, K.B. Davis, M.A. Joffe, A. Martin, D.E. Pritchard, *Phys. Rev. Lett.* **70**, 2253 (1997).
21. S. Friebe, C. D'Andrea, J. Walz, M. Weitz, and T.W. Hänsch, *Phys. Rev. A* **57**, R20 (1998).
22. N. N. Klausen, J. L. Bohn, and C. H. Greene, *Phys. Rev. A* **64**, 053602 (2001); E. G. M. van Kempen, S. J. J. M. F. Kokkelmans, D. J. Heinzen, and B. J. Verhaar, *Phys. Rev. Lett.* **88**, 093201 (2002).
23. R. Grimm, private communication.
24. R. Scheunemann, F.S. Cataliotti, T.W. Hänsch, M. Weitz, *Phys. Rev. A* **62**, 51801 R, (2000).
25. D. Jaksch, H.-J. Briegel, J.I. Cirac, C.W. Gardiner, and P. Zoller, *Phys. Rev. Lett.* **82**, 1975 (1999).

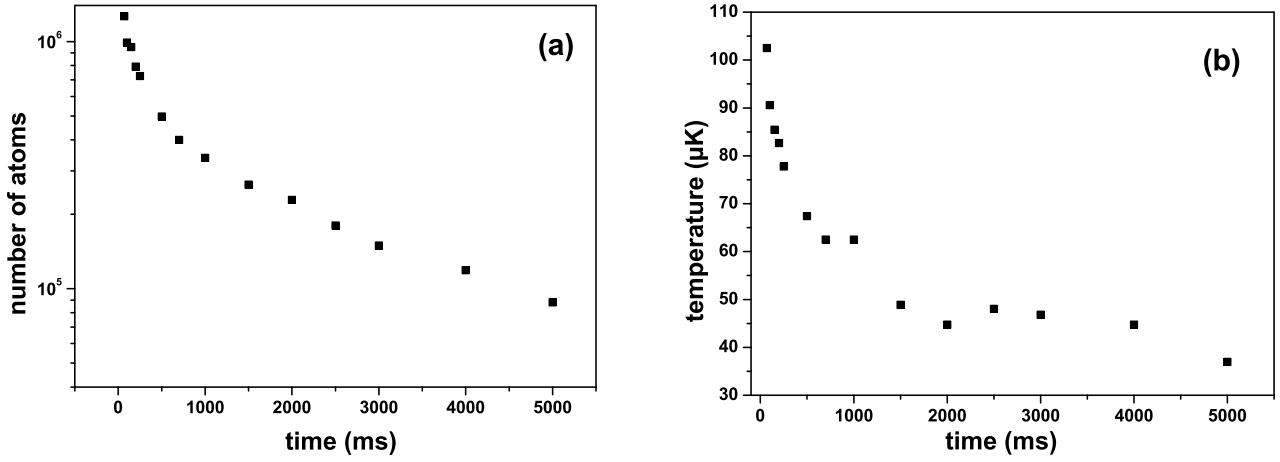


Fig. 2 (a): Number of trapped atoms and (b) atomic temperature versus trapping time in a CO₂-laser crossed dipole trap configuration.

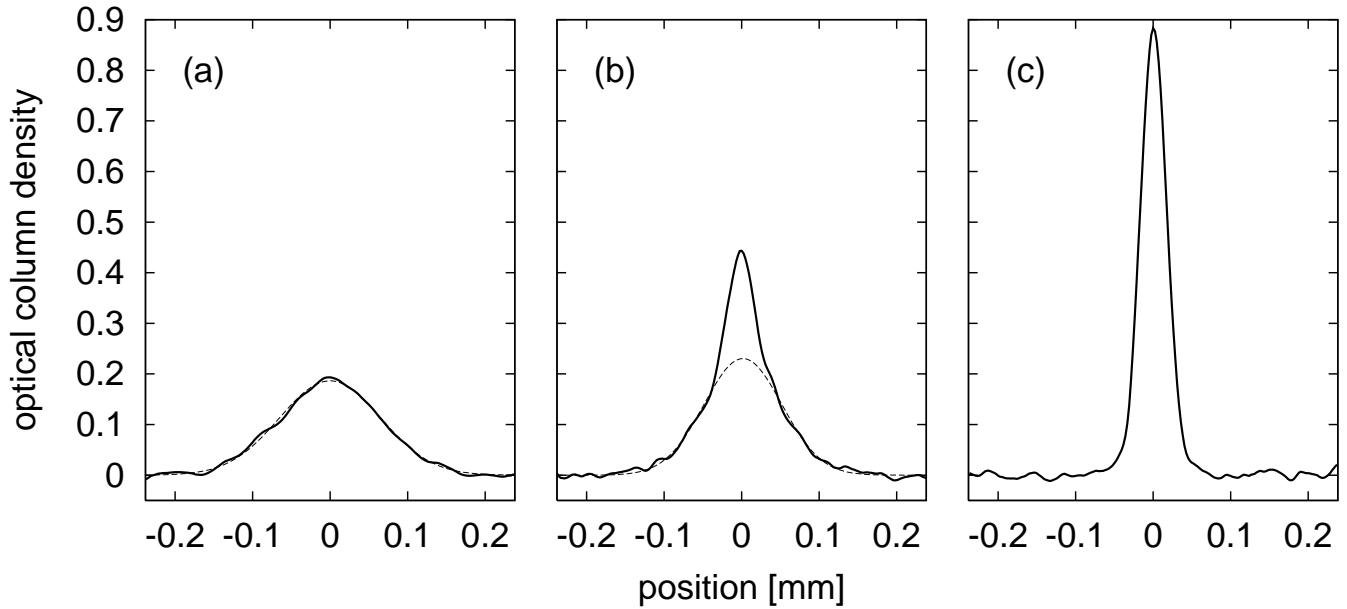


Fig. 3 Formation of a Bose-Einstein condensate in a crossed beam dipole trap. The plots show density profiles for (a) a final trapping beam power of 150 mW, yielding a thermal cloud corresponding to a temperature of 240 nK. (b) Final ramp power of 100 mW, yielding an atomic temperature of 200 nK. This value is near the critical temperature of 190 nK. A bimodal distribution with the central feature corresponding to Bose-condensed atoms and a thermal atomic distribution in the wings is visible. (c) Data taken at for final ramp power of 75 mW. An almost pure Bose-Einstein condensate is here produced.

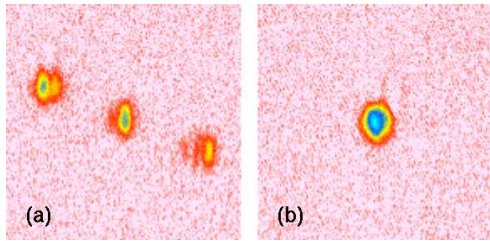


Fig. 5 Shadow images of Bose-Einstein condensates generated in a single beam dipole trap after allowing 15 ms of free expansion, see also [15]. The field of view comprises $380\ \mu\text{m} \times 380\ \mu\text{m}$. (a) Stern-Gerlach magnetic field applied only during the free expansion phase. The three components $m_F = \pm 1, 0$ of a spinor condensate have separated into three spatially resolved clouds. (b) Stern-Gerlach field activated during the evaporative cooling phase. Here, a pure $m_F = 0$ condensate is generated.